

Interlamellar Chemistry of Hydrotalcites

I. Polymerization of Silicate Anions

A. SCHUTZ* AND P. BILOEN†

Department of Chemical and Petroleum Engineering, University of Pittsburgh, Pittsburgh, Pennsylvania 15261

Received July 21, 1986; in revised form October 8, 1986

Exchange of silicate anions into hydrotalcite-type materials leads to the ready formation of well-ordered two-dimensional silicate sheets. The combined evidence from diffraction, NMR, and IR allows for a global identification of the reaction product. Its structure probably consists of positively charged brucitelike layers intercalated with puckered, silicic-acid-type macroanions. © 1987 Academic Press, Inc.

1. Introduction

Hydrotalcitelike materials are mixed metal hydroxides, with the generic formula $[M_{1-x}^{II} M_x^{III} (\text{OH})_2]^{x+} Y_{x/z}^{z-} \cdot n\text{H}_2\text{O}$ (1, 2). Their structure consists of positively charged brucite-type layers, $M(\text{OH})_2$, separated by intercalated, charge-balancing anions (3, 4). This structure is chargewise the mirror image of widely studied cation exchangers, such as clays (5) and zirconium phosphates (6). The rather unique charge organization in hydrotalcites has prompted us into a systematic study of their intercalation chemistry. The present report deals with the intercalation chemistry of silicate anions.

2. Experimental

Materials Synthesis

Silication involved two different hydrotalcite-type starting materials, i.e., $[\text{Mg}_3\text{Al}(\text{OH})_8]^+\text{Cl}^-$ and $[\text{Al}_2\text{Li}(\text{OH})_6]^+\text{Cl}^-$.

* To whom all correspondence should be addressed.

† Deceased.

$[\text{Mg}_3\text{Al}(\text{OH})_8]^+\text{Cl}^-$ was prepared by room-temperature precipitation of stoichiometric amounts of Al^{3+} and Mg^{2+} with NaOH at $\text{pH} \approx 8.5$. After a hydrothermal treatment at 220°C for 18 hr one obtains hexagonal platelike crystals with lateral dimensions between 1 and $2 \mu\text{m}$ and a thickness around $0.1 \mu\text{m}$ (Fig. 1A).

$[\text{Al}_2\text{Li}(\text{OH})_6]^+\text{Cl}^-$ was prepared by reacting Gibbsite, $\text{Al}(\text{OH})_3$, for 18 hr at room temperature with 1 M LiCl (7). The resulting material exhibits an XRD pattern identical to that reported in (8, 9). The aforementioned references contain the justification for classifying $[\text{Al}_2\text{Li}(\text{OH})_6]^+\text{Cl}^-$ as a hydrotalcite-type material.

A silicate-anion-containing solution was prepared by suspending 2 g amorphous silicic acid (Baker Analyzed Reagent, SiO_2) into 200 ml of a 0.05 M NaOH solution. After 10 min of agitation, 1 g of either $[\text{Mg}_3\text{Al}(\text{OH})_8]^+\text{Cl}^-$ or $[\text{Al}_2\text{Li}(\text{OH})_6]^+\text{Cl}^-$ was added to the suspension, and the stirred mixed suspension was subsequently refluxed for 18 hr at 100°C . The pH went

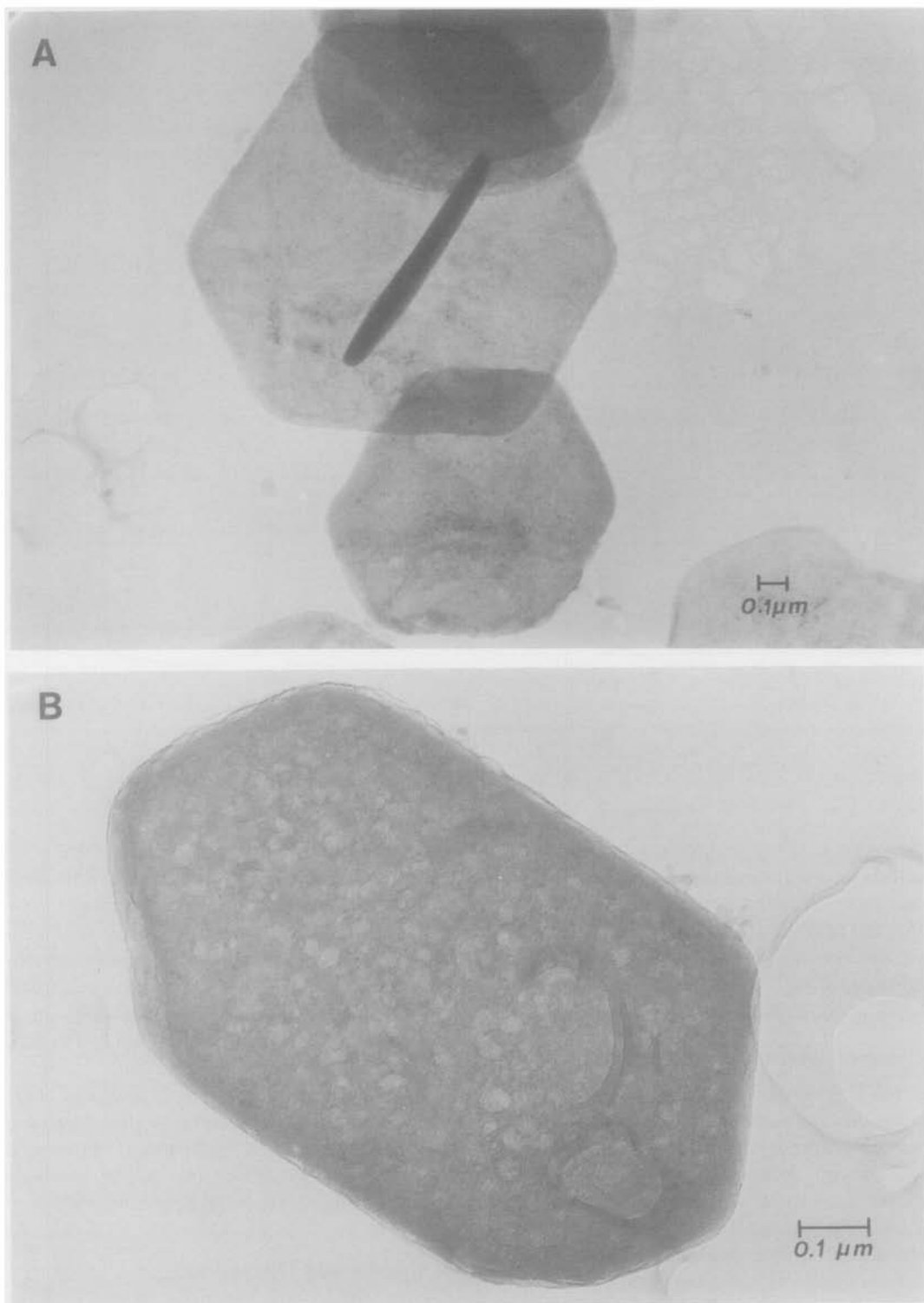


FIG. 1. (A) (TEM) The starting material, $[\text{Mg}_3\text{Al}(\text{OH})_8]^+\text{Cl}^-$, exhibits a narrow size distribution. The hexagonal plates have lateral dimensions between 1 and 2 μm and a thickness around 0.1 μm . The plates are single crystals (cf. Fig. 5A). (B) Silication doesn't affect the TEM, i.e., the reaction is a topotactical one.

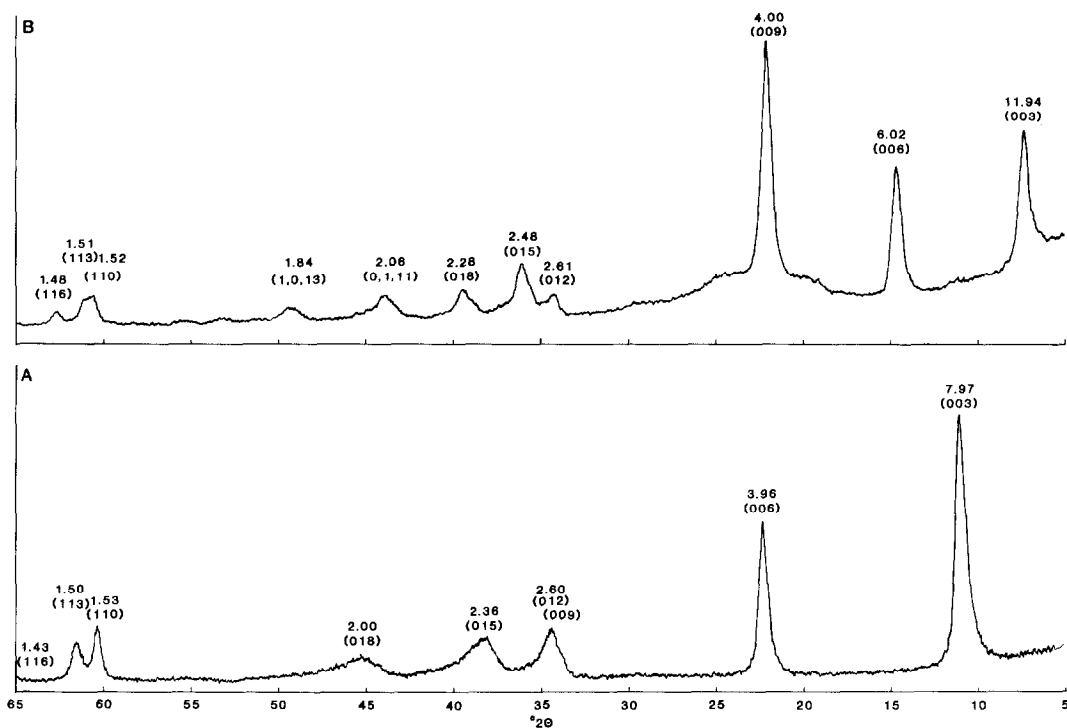


FIG. 2. XRD of $[\text{Mg}_3\text{Al}(\text{OH})_8]^+\text{Cl}^-$ before (A) and after (B) silication. The change in basal reflections is complete after 18 hr reaction time.

down from 10 to 9 during silication (room-temperature-recorded values). The reaction products were collected by decantation, leaving unreacted silica at the bottom. Prior to further analyses, the reaction products were washed by centrifugation and dried for 8 hr at 75°C.

Physical Characterization

XRD patterns ($\text{CuK}\alpha$) were recorded on a powder diffractometer (GE-700) equipped with a graphite monochromator.

Electron diffraction patterns and TEM pictures were obtained with a JEOL 200CX TEM. The samples were prepared by drying a drop of the diluted suspension at ambient conditions on a carbon-coated copper grid. Electron-beam-induced sample degradation was not observed.

High-resolution ^{27}Al and ^{29}Si NMR spec-

tra were obtained with a Bruker MSL-300 spectrometer (^{27}Al : 78.17 MHz; ^{29}Si : 59.4 MHz) utilizing magic angle spinning.

The sample preparation for IR spectroscopy consisted of diluting 10 mg of the samples into 1 g kBr. IR spectra were recorded in the spectral domain of 1000–4000 cm^{-1} utilizing a wavelength-dispersive instrument (Perkin-Elmer 683).

X-ray fluorescence analysis was performed in the microprobe mode utilizing a JEOL 35CF SEM instrument equipped with an energy-dispersive X-ray analysis system (TRACOR NORTHERM 2000).

3. Results and Discussion

The presentation of the results focuses largely on silication of $[\text{Mg}_3\text{Al}(\text{OH})_8]^+\text{Cl}^-$. The silication results for $[\text{Al}_2\text{Li}(\text{OH})_6]^+\text{Cl}^-$

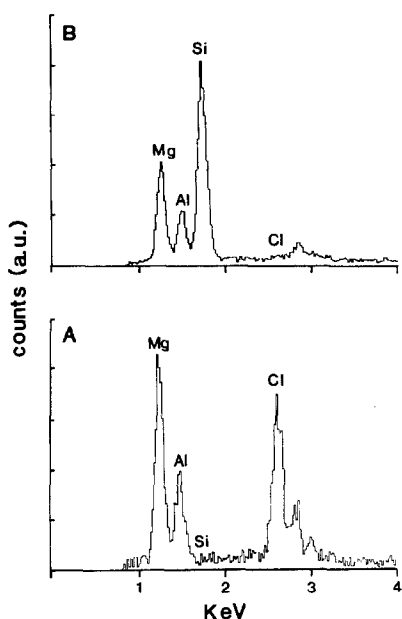


FIG. 3. Microprobe analysis before (A) and after (B) silication. Cl is being replaced by Si. The Mg/(Mg + Al) ratio doesn't change upon silication.

are very similar, confirming the hydrotalcite-type structure of this material (8, 9) and suggesting that the presently reported results are transferable to other hydrotalcite-type materials.

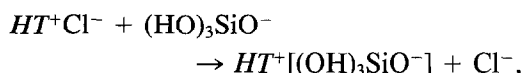
The reaction between $[\text{Mg}_3\text{Al}(\text{OH})_8]^+\text{Cl}^-$ and soluble silica proceeds rapidly to completion, as shown in XRD by the change in basal reflections (Figs. 2A and 2B). The change in XRD pattern is virtually complete after only 1 hr of reflux.

Microprobe analysis (Fig. 3) shows that the reaction leads to a quantitative displacement of Cl^- by a silicon-containing species. In what follows we therefore refer to the reaction as a "silication" reaction.

Several observations indicate independently that the structure of the $[\text{Mg}_3\text{Al}(\text{OH})_8]^+$ layers survive the silication intact. TEM (Figs. 1A and 1B) indicates the reaction to be a topotactical one, in that the lateral dimensions of the hexagonal plates are not affected by silication. The Al/(Al +

Mg) ratio remains constant, as shown by microprobe analysis (Fig. 3). The ^{27}Al -NMR (Figs. 4A and 4B) shows Al before and after silication to be located in the octahedral coordination, which is characteristic of the $[\text{Mg}_3\text{Al}(\text{OH})_8]^+$ structure. The ^{29}Si -NMR (Fig. 6) conveys a lack of Si-O-Al bond formation as a single peak at -104 ppm is being observed.

Evidence so far is compatible with a "straightforward" anion-exchange reaction, for example,



in which $\text{HT}^+ = [\text{Mg}_3\text{Al}(\text{OH})_8]^+$, $[\text{Al}_2\text{Li}(\text{OH})_6]^+$. Revealing evidence, however, is being provided by electron diffraction

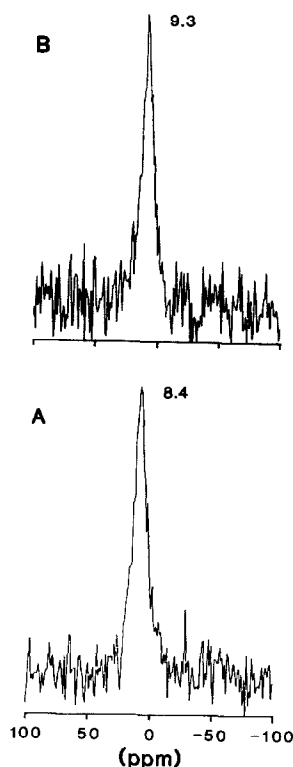


FIG. 4. ^{27}Al -MAS-NMR before (A) and after (B) silication. The line position, referenced to $\text{Al}(\text{H}_2\text{O})_6^{3+}$, is characteristic of octahedrally coordinated Al^{3+} .

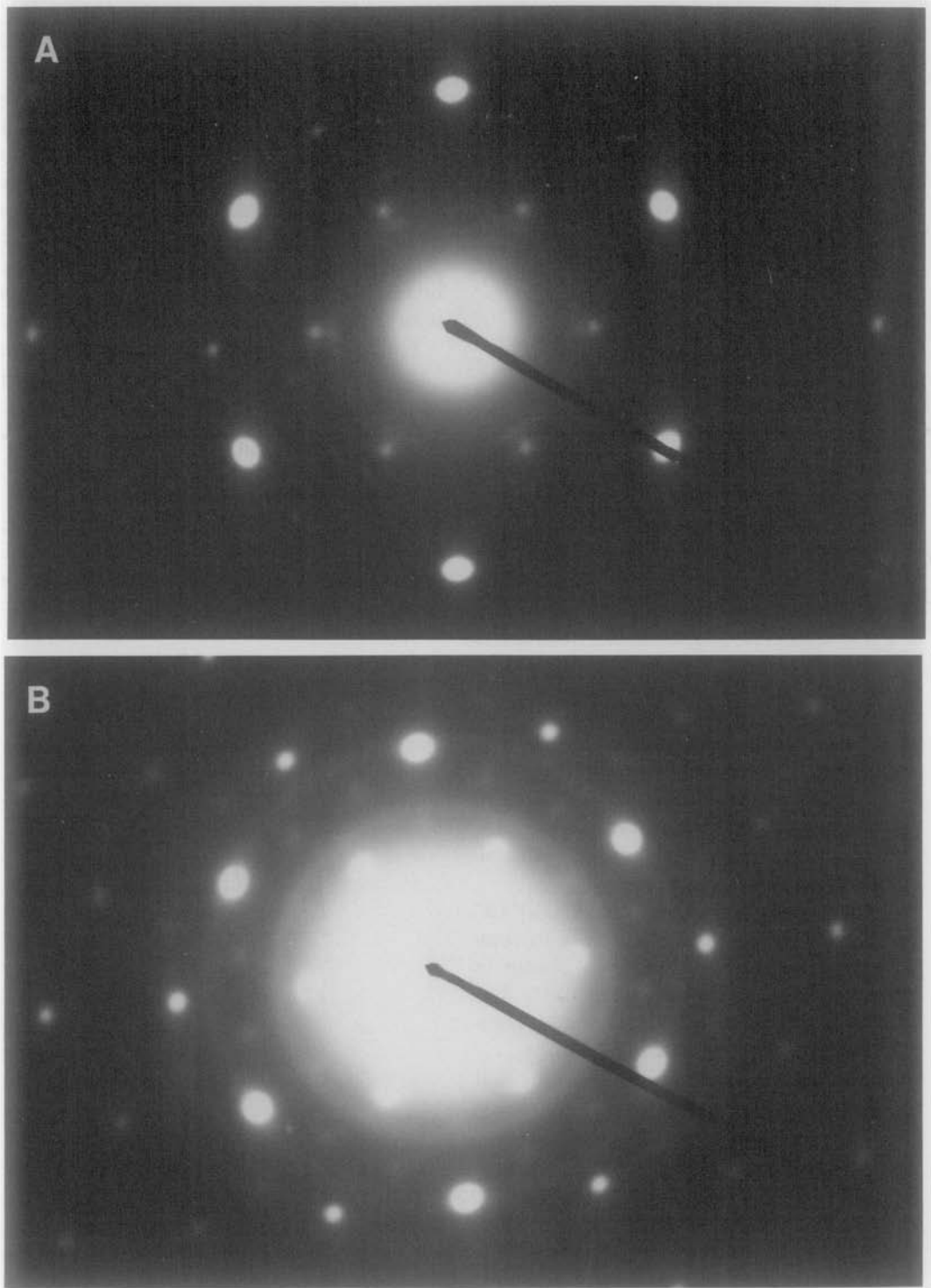


FIG. 5. Electron diffraction before (A) and after (B) silication. Electron beam diameter is approximately $1\ \mu\text{m}$, with the beam parallel to the $[001]$ direction. Silication leads to a superstructure with $5.2\text{-}\text{\AA}$ repeat distance.

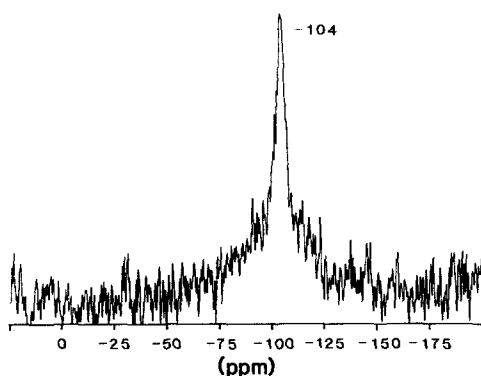


FIG. 6. ^{29}Si -MAS-NMR of silicated $[\text{Mg}_3\text{Al}(\text{OH})_8]^+\text{Cl}^-$. The chemical shift is characteristic of Q_3 (oAl) silicon. Reference is $\text{Si}(\text{CH}_3)_4$.

(Figs. 5A and 5B). With the electron beam (beam diameter approximately $1\ \mu\text{m}$) parallel to the [001] direction and the selected

area approximately equal to the size of the hexagonal plates, both the starting material (Fig. 5A) and the product (Fig. 5B) behave as single crystalline. The diffraction pattern of the starting material is characteristic of a hexagonal closed-packed hydroxide layer, with $a = b = 3.06\ \text{\AA}$ (10). Silication results in a superstructure characteristic of a two-dimensional hexagonal unit cell with $a = b = 5.2\ \text{\AA}$ (Fig. 5B). A hexagonal unit cell of this dimension is characteristic of a flat zweier silicate layer in phyllosilicates (11), with $5.2\ \text{\AA}$ being the repeat distance between the six-membered Si-O-Si rings.

Further evidence for the well-organized nature of the intercalated silica is provided by ^{29}Si -NMR (Fig. 6). The sharp resonance at $-104\ \text{ppm}$ (relative to $\text{Si}(\text{CH}_3)_4$) compares well with that of talc ($-98\ \text{ppm}$ (12))

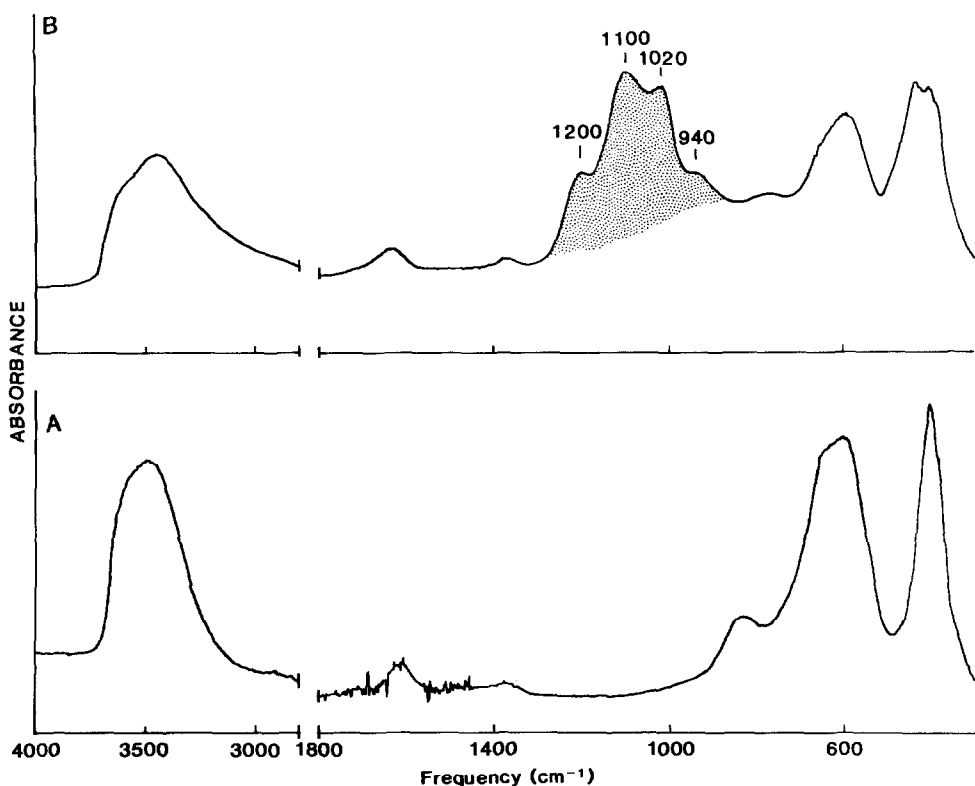


FIG. 7. IR before (A) and after (B) silication. The 1200-cm^{-1} band in the Si-O bands is assigned to a Si-O-Si bond angle of 180° .

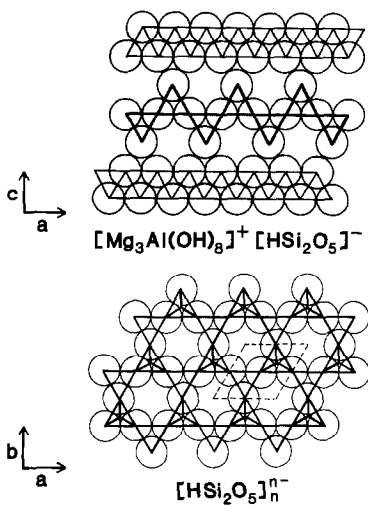


FIG. 8. The proposed structure is that of a puckered two-dimensional silicate anion intercalated between positively charged brucite sheets. Approximately 50% of the terminal groups are SiOH and the other 50% SiO^- (as required by charge balance).

and synthetic sodium silicate (-102 ppm (13)). From the data presented in Table II of Ref. (15) (Janes and Oldfield) we find -104 ppm to be outside the range observed for $Q^4(\text{oAl})$ and to be compatible with $Q^3(\text{oAl})$ at a Si-O-Si bond angle higher than 140° . The NMR behavior reflects a two-dimensional structure of macroscopic dimensions (i.e., with only a small fraction of edge atoms), with all silicon atoms being isostructural and bonded to three other silicons via bridging oxygens.

Further information regarding the structure of the intercalated silicate layer is being provided by infrared spectroscopy (Fig. 7). Silication leads to a well-developed band around $1100\text{--}1000\text{ cm}^{-1}$, as commonly observed in layered silicates (14). Noteworthy, however, is the pronounced structure at the high-energy side of the band, i.e.,

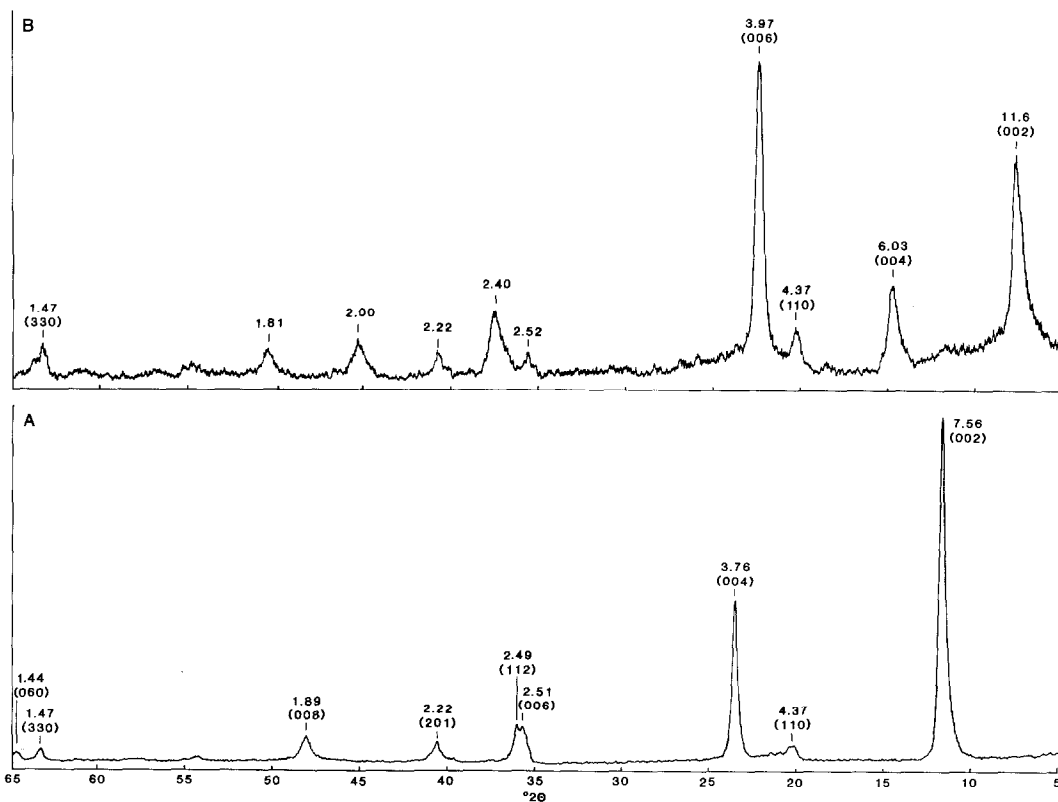


FIG. 9. XRD of $[\text{Al}_2\text{Li}(\text{OH})_6]^+\text{Cl}^-$ before (A) and after (B) silication.

around 1200 cm^{-1} . From general valence force considerations, one expects the frequency of Si–O–Si vibrations to increase with increasing Si–O–Si bond angle. As shown by the IR spectra of sepiolite or antigorite (14), the 1200-cm^{-1} position corresponds to a 180° Si–O–Si bond angle.

The aforementioned leads us to propose for the silicate-intercalated product a schematic overall structure as depicted in Fig. 8. A summary of the essential features of the proposed structure and the supporting evidence is given below.

1. The brucite layer structure and charge remain intact: TEM (topotactic reaction), microprobe (retention of the Al/(Al + Mg) ratio), ^{27}Al -NMR (Al^{3+} remains in octahedral coordination), ^{29}Si -NMR ($Q_3(\text{oAl})$, i.e., no Al–O–Si bond formation), IR (the material retains the majority of its OH groups), electron diffraction (ac-

commodating a 3.04-\AA unit cell, characteristic of hexagonal OH layers), and XRD (a 12.0-\AA basal spacing, compatible with 4.8 \AA for the brucite layer and 7.2 \AA for puckered silicic acid; see below).

2. The Cl^- anions have been replaced by anionic silica: microprobe analysis.

3. The silicate is condensed into a two-dimensional six-ring structure of macroscopic dimensions: electron diffraction and ^{29}Si -NMR.

4. The silicate layer has a puckered configuration: IR (the 1200-cm^{-1} bond, corresponding to a Si–O–Si bond angle of 180°) and XRD (an interlayer spacing of 7.2 \AA) both indicate a puckered configuration.

Silication of $[\text{Al}_2\text{Li}(\text{OH})_6]^+\text{Cl}^-$ leads to virtually identical results (Figs. 9 and 10). This suggests that the presently reported reaction is of a more general nature. One of the intriguing aspects of this reaction is its

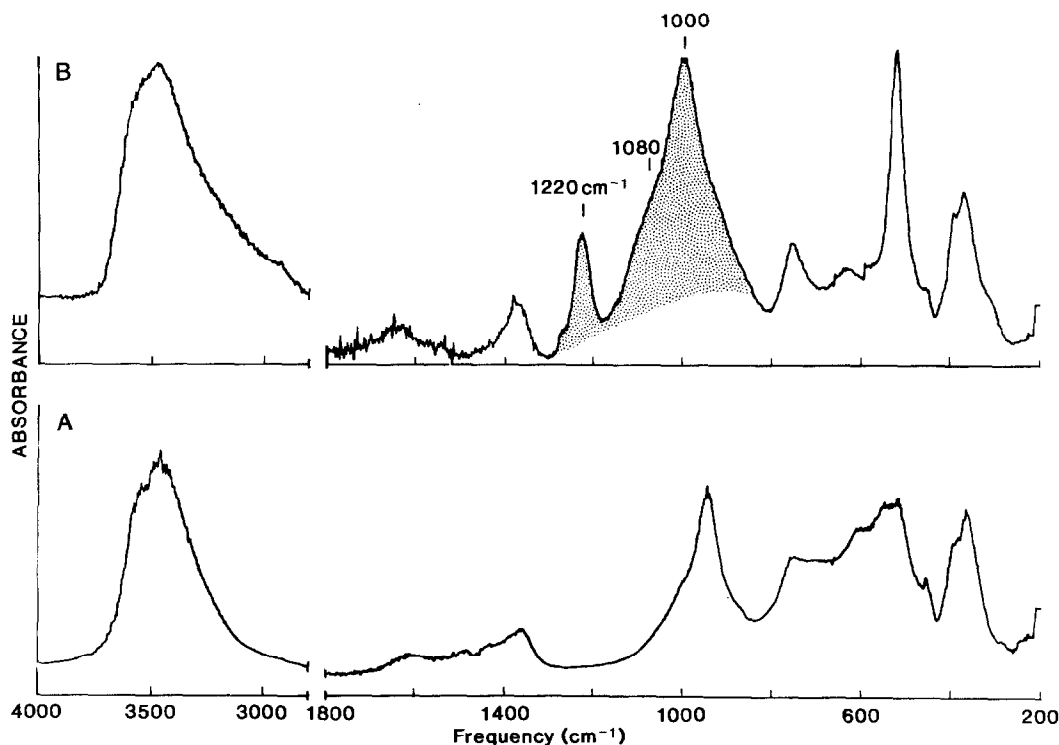


FIG. 10. IR before (A) and after (B) silication of $[\text{Al}_2\text{Li}(\text{OH})_6]^+\text{Cl}^-$.

possible implication for the low-temperature synthesis of novel di- and trioctahedral clay-type materials. This aspect currently is under investigation.

Acknowledgments

Guidance in the diffraction and microscopy measurements was provided by the staff of our Material Science and Engineering Department. Financial support of the U.S. Department of Energy (Contract DE-FG22-84PC 70808), the Exxon Education Foundation, and U.S. Steel Chemicals is gratefully acknowledged.

References

1. S. MIYATA, *Clays Clay Miner.* **31**, 305 (1983).
2. H. F. W. TAYLOR, *Mineral Mag.* **39**, 377 (1973).
3. R. ALLMANN, *Acta Crystallogr. Sect. B* **24**, 972 (1968).
4. D. L. BISH, *Bull. Mineral.* **103**, 170 (1980).
5. G. W. BRINDLEY, in "Crystal Structure of Clay Minerals and Their X-Ray Identification," Mineralogical Society, London (1980).
6. A. CLEARFIELD, in "Inorganic Ion Exchange Materials," Chem. Rubber Co., Cleveland (1982).
7. C. WILLIAM *et al.*, U.S. Patent 4,348,296 (1982).
8. I. SISSOKO, E. T. IYAGBA, R. SAHAI, AND P. BILOEN, *J. Solid State Chem.* **60**, 283 (1985).
9. C. J. SERNO, J. L. RENDON, AND J. E. IGLESIAS, *Clays Clay Miner.* **30**, 3 180 (1982).
10. A. F. WELLS, in "Structural Inorganic Chemistry," Oxford Univ. Press (Clarendon), London/New York (1984).
11. F. LIEBAU, in "Structural Chemistry of Silicates," Springer-Verlag, New York/Berlin (1985).
12. R. A. KINSEY, R. J. KIRKPATRICK, J. HOWER, K. A. SMITH, AND E. OLDFIELD, *Amer. Mineral.* **70**, 537 (1985).
13. W. SCHWIEGER, D. HEIDEMANN, AND K. H. BERGK, *Rev. Chim. Miner.* **22**, 639 (1985).
14. A. N. LAZAREV, in "Vibrational Spectra and Structure of Silicates," C/B Consultants Bureau, New York/London (1972).
15. N. JANES AND E. OLDFIELD, *J. Amer. Chem. Soc.* **107**, 6769 (1985).